CORTEX 129 (2020) 41–56

Available online at www.sciencedirect.com

ScienceDirect

Journal homepage: www.elsevier.com/locate/cortex

Research Report

Intrinsic functional architecture of the human speech processing network

Daniel A. Abrams [a,*], *John Kochalka* [a], *Sayuli Bhide* [a], *Srikanth Ryali* [a] *and Vinod Menon* [a,b,c,**]

[a] *Department of Psychiatry and Behavioral Sciences, Stanford University School of Medicine, Stanford, CA, USA*
[b] *Program in Neuroscience, Stanford University School of Medicine, Stanford, CA, USA*
[c] *Department of Neurology and Neurological Sciences, Stanford University School of Medicine, Stanford, CA, USA*

ARTICLE INFO

Article history:
Received 9 October 2019
Reviewed 26 November 2019
Revised 12 February 2020
Accepted 26 March 2020
Action editor Sonja Kotz
Published online 21 April 2020

Keywords:
Auditory cortex
Speech
Inferior frontal gyrus
Angular gyrus
Superior temporal sulcus

ABSTRACT

Speech engages distributed temporo-fronto-parietal brain regions, however a comprehensive understanding of its intrinsic functional network architecture is lacking. Here we investigate the human speech processing network using the largest sample to date, high temporal resolution resting-state fMRI data, network stability analysis, and theoretically informed models. Network consensus analysis revealed three stable functional modules encompassing: (1) superior temporal plane (STP) and Area Spt, (2) superior temporal sulcus (STS) + ventral frontoparietal cortex, and (3) dorsal frontoparietal cortex. The STS + ventral frontoparietal cortex module showed the highest participation coefficient, and a hub-like organization linking STP with frontoparietal cortical nodes. Node-wise analysis revealed key connectivity features underlying this modular architecture, including a leftward asymmetric connectivity profile, and differential connectivity of STS and STP, with frontoparietal cortex. Our findings, replicated across cohorts, reveal a tripartite functional network architecture supporting speech processing and provide a novel template for future studies.

1. Introduction

Brain structures engaged during speech processing consist of unimodal auditory structures in superior temporal cortex (STC), encompassing Heschl's gyrus (HG), planum temporale (PT), and lateral superior temporal gyrus (STG), multimodal structures in superior temporal sulcus (STS), and heteromodal structures within anterior temporal lobe (ATL), inferior parietal, and prefrontal cortices (Tyler & Marslen-Wilson, 2008).

* *Corresponding author*. Stanford Cognitive and Systems Neuroscience Lab, Department of Psychiatry and Behavioral Sciences, Stanford University, 1070 Arastradero Road, Suite 220, Palo Alto, CA, 94304-1345, USA.
** *Corresponding author*. Stanford Cognitive and Systems Neuroscience Lab, Department of Psychiatry and Behavioral Sciences, Stanford University, 1070 Arastradero Road, Suite 220, Palo Alto, CA, 94304-1345, USA.
E-mail addresses: daa@stanford.edu (D.A. Abrams), menon@stanford.edu (V. Menon).
https://doi.org/10.1016/j.cortex.2020.03.013
0010-9452/

Abbreviations

STP	superior temporal plane
STS	superior temporal sulcus
STC	superior temporal cortex
HG	Heschl's gyrus
PT	planum temporale
STG	superior temporal gyrus
ATL	anterior temporal lobe
IFG	inferior frontal gyrus
POp	pars opercularis
PTri	pars triangularis
POrb	pars orbitalis
SMG	supramarginal gyrus
IPL	inferior parietal lobule
MC	motor cortex
AG	angular gyrus
vFP	ventral frontoparietal
dFP	dorsal frontoparietal

These brain areas have long been implicated in speech processing based on neuropsychological evaluations in patients with focal lesions of the cortex which have implicated left-hemisphere temporal (Wernicke, 1874) and parietal regions (Geschwind, 1970) as well as prefrontal contributions associated with classically defined Broca's area (Bates et al., 2003). Functional neuroimaging has provided corroborating evidence that a distributed left-hemisphere network involving the superior temporal, inferior parietal, and inferior frontal gyrus (IFG) underlie speech processing (Peelle, Johnsrude, & Davis, 2010; Price, 2010; Tyler & Marslen-Wilson, 2008). Importantly, a number of factors in previous studies have precluded a more comprehensive understanding of the organization of the speech processing network, including the use of small sample sizes, a lack of comprehensive replication analyses, and a focus on regional activation profiles rather than network measures. Despite the overwhelming evidence implicating multiple temporo-fronto-parietal regions for speech processing (Fridriksson et al., 2016; Peelle et al., 2010; Price, 2010), little is known regarding the large-scale network organization of these brain structures.

Several theoretical models have been proposed to describe functional cortical pathways linking STC and heteromodal target regions associated with speech processing (Binder, Desai, Graves, & Conant, 2009; Friederici, 2012; Hickok & Poeppel, 2007; Price, 2010; Rauschecker & Scott, 2009; Turken & Dronkers, 2011; Tyler & Marslen-Wilson, 2008). However, the functional architecture elaborated by these models diverge both at the level of the STC and their frontal and parietal targets. An important hypothesis emerging from these models is that temporo-fronto-parietal structures diverge into two streams of processing in a manner similar to dorsal-ventral visual processing streams (Mishkin, Ungerleider, & Macko, 1983). However, different auditory "dual stream" models have specified divergent anatomical configurations for these processing streams (Bornkessel-Schlesewsky, Schlesewsky, Small, & Rauschecker, 2015; Hickok & Poeppel, 2007; Rauschecker & Scott, 2009). For example, an influential model proposed by Rauschecker and Scott (Rauschecker & Scott, 2009) is based on seminal research (Rauschecker & Tian, 2000; Scott, Blank, Rosen, & Wise, 2000) and posits that auditory processing streams diverge from auditory cortex into: (i) an antero-ventral path, which extends anteriorly from the STC into the inferior frontal gyrus (IFG) regions pars opercularis (POp; Brodmann Area 44) and pars triangularis (PTri; Brodmann Area 45), and (ii) a postero-dorsal path, which extends posteriorly from auditory cortex into supramarginal gyrus (SMG) of the inferior parietal lobule (IPL). These streams are hypothesized to serve sound-to-meaning and auditory spatial processing, respectively.

A different dual-stream model proposes a different orientation of processing streams (Hickok & Poeppel, 2007). This model specifies: (i) a ventral stream encompassing a broad extent of temporal cortex, and (ii) a sensorimotor dorsal stream, which includes frontoparietal brain systems instantiated in POp and PTri, motor cortex (MC), and lateral IPL. These streams are hypothesized to serve sound-to-meaning and sensorimotor processing, respectively. A critical facet of this model is the identification of a temporoparietal region, Area Spt, a brain region bordering the PT and infero-lateral parietal cortex that was first identified in a study showing that Area Spt is activated during both phonological perception and production tasks (Buchsbaum, Hickok, & Humphries, 2001), suggesting a key role in sensory motor integration of speech. Another study provided important information regarding a potential role for Area Spt in connecting temporo-frontal brain regions. This study examined perceptual and phonological-articulatory aspects of verbal working memory and results revealed increased task-based functional connectivity between Area Spt and dorsal aspects of prefrontal cortex (Buchsbaum, Olsen, Koch, & Berman, 2005). Consequently, the Hickok and Poeppel dual stream model (Hickok & Poeppel, 2007) attributes a primary role for Area Spt in connecting superior temporal and inferior parietal regions to dorsal aspects of IFG and MC (Buchsbaum et al., 2005).

Other models have proposed different configurations for the cortical speech comprehension network. For example, evidence from meta-analyses of speech and language comprehension studies (Binder et al., 2009; Price, 2010), voxel-based lesion-symptom mapping (Bates et al., 2003; Dronkers, Wilkins, Van Valin, Redfern, & Jaeger, 2004), and structural connectivity (Saur et al., 2008) have not only highlighted a different collection of structures within the STC underlying speech processing but have also specified a different set of prefrontal and inferior parietal nodes in this network. These models place a greater emphasis on distinctions in the superior-to-inferior plane of STC, with a more central role for the STS in the inferior aspects of STC compared to HG, PT and other structures of the STP. Moreover, these models identify pars orbitalis subdivision of the IFG (POrb; Brodmann Area 47) and the angular gyrus (AG) subdivision of IPL as key targets of the STS for speech comprehension.

An important factor contributing to the inconsistency of extant models has been a lack of comprehensive high-temporal resolution samples and methods for characterizing the functional organization of this extensive cortical network. However, research in other cognitive domains has shown that

precise quantitative characterization of functional brain networks can provide novel insights into the organization of these networks (Bressler & Menon, 2010; Bullmore & Sporns, 2009; Cai, Ryali, Chen, Li, & Menon, 2014; Greicius, Krasnow, Reiss, & Menon, 2003; Power et al., 2011; Seeley et al., 2007). Importantly, applying these methods to the speech processing network may provide critical new insights into the functional architecture of this cognitive network.

The goal of the current study is to address critical gaps in our knowledge of the functional architecture of human speech processing network and test competing models of cortical speech processing. We first used network stability analysis of resting-state fMRI data to probe the modular organization of the speech comprehension network. To better understand the specific network features that contribute to its modular organization, we then investigated intrinsic (resting-state) connectivity of STP and STS subdivisions of the STC, as well as the connectivity of STC along its anterior-posterior axis, with multiple prefrontal and parietal targets implicated in speech comprehension. We used these analytic techniques to address five primary questions: (1) What is the community structure of this network?; (2) Are there specific links in this network that facilitate communication between functionally-defined modules? (3) Do different STC sub-regions, including STP and STS, show distinct connectivity profiles? (4) What are the primary prefrontal and parietal targets of the STC?; and, (5) Does connectivity between the STC and IFG and IPL targets vary as a function of spatial proximity or cerebral hemisphere? Importantly, we overcome crucial limitations in previous studies by using the largest sample to date in the speech processing literature ($N > 250$), high temporal resolution fMRI data from the HCP (Van Essen et al., 2013), comprehensive replication analysis (Cai et al., 2014; Supekar et al., 2013), and theoretically informed models.

2. Results

With the goal of presenting and highlighting reproducible results, only results replicated in both primary and replication cohorts are reported and discussed.

2.1. Network analysis

The first goal of the study was to use graph theoretic measures to investigate the network structure of auditory functional pathways linking STC with IFG and IPL. The nodes included in this analysis consisted of STP and STS nodes extending from posterior STC through temporal pole, prefrontal nodes of IFG and MC, and inferior parietal nodes, including aSMG and AG (Figs. 1a and 2a for node locations). Results for the primary and replication cohorts were extremely similar, with below-diagonal values in the connectivity matrices for primary and replication cohorts (Fig. 1c, d) showing a correlation of $r = .96$ ($p = 2.81 \times 10^{-64}$).

Community detection analysis for both primary and replication cohorts revealed that the 16 fronto-temporo-parietal nodes in the speech processing network formed three distinct communities: (1) an STP plus Area Spt module (STP + Spt), (2) an STS plus ventral frontoparietal (vFP) module, which included all STS nodes, POrb, and PGp (STS + vFP), and (3) a dorsal frontoparietal (dFP) module that consisted of POp, PTri, and MC of frontal cortex and aSMG and PGp of parietal cortex (Fig. 1a, b). The weighted connectivity matrices (Fig. 1c, d) show strong dissociation between STP and STS nodes of the network, further highlighting distinctions between these aspects of STC, and further show that the STS + vFP module has greater inter-modular communication with the dFP module (see bottom center section of the connectivity matrices) compared to the STP + Spt module (bottom left section of the matrices). We computed the normalized participation coefficient for each node and then within each community in the network for each participant (see Methods). Results reveal that the STS + vFP community has the greatest normalized participation coefficient among the three communities (Fig. 1e, f; $p < .0001$ for both primary and replication cohorts), suggesting that it plays a hub-like role in the speech processing network. Together, results from graph theoretic analysis shows that: (1) the community structure of the speech processing network consists of STP + Spt, STS + vFP, and dFP communities; and (2) the STS + vFP community has the greatest normalized participation coefficient among the three communities, suggesting that it serves as a hub that links auditory processing structures of STC with dorsal heteromodal regions of IFG and IPL.

2.2. Node-wise functional connectivity analysis along the anterior-posterior axis of STP, STS, and Area Spt

The next goal of the analysis was to conduct fine-grained analysis of connectivity profiles along the anterior-posterior axis of STP and STS. This allowed us to probe the functional organization of the STP and STS and identify features underlying the network results (Fig. 1). Functional connectivity analyses were performed using four adjacent seeds within the STP (Fig. 2b, left) as well as four adjacent nodes within the STS (Fig. 2c, left). Together, these eight ROIs encompass a broad anterior-posterior expanse of both STP and STS subregions to enable a fine-grained analysis of connectivity profiles in STC. Connectivity strength between each of these seeds and prefrontal (POp, PTri, POrb, and MC) and parietal targets (aSMG, PGa, and PGp) were then entered into an omnibus $2 \times 4 \times 7$ RMANOVA (STC subregion x Anterior-posterior STC seed location x Prefrontal/Parietal targets; see SI Fig. 1 for RMANOVA schematic and results). All seeds and targets in this initial RMANOVA were located in the left-hemisphere.

2.2.1. Main Effects

For both primary and replication cohorts, results showed a strong main effect of STC subregion, with the STS subregion showing greater connectivity strength compared to the STP [primary cohort: $F(1, 122) = 185.93$, $p < .0001$; Partial $Eta^2 = .60$; replication cohort: $F(1, 135) = 179.43$, $p < .0001$; Partial $Eta^2 = .57$; see SI Fig. 1 for RMANOVA schematic and results]. There was also a main effect of seed location along the anterior-posterior axis of the STC [primary cohort: $F(3, 366) = 22.99$ $p < .0001$; replication cohort: $F(3, 405) = 16.66$, $p < .0001$], and pairwise comparisons showed that the pSTC seeds had greater overall connectivity compared to pmSTC, amSTC, and aSTC seeds (primary and replication cohorts:

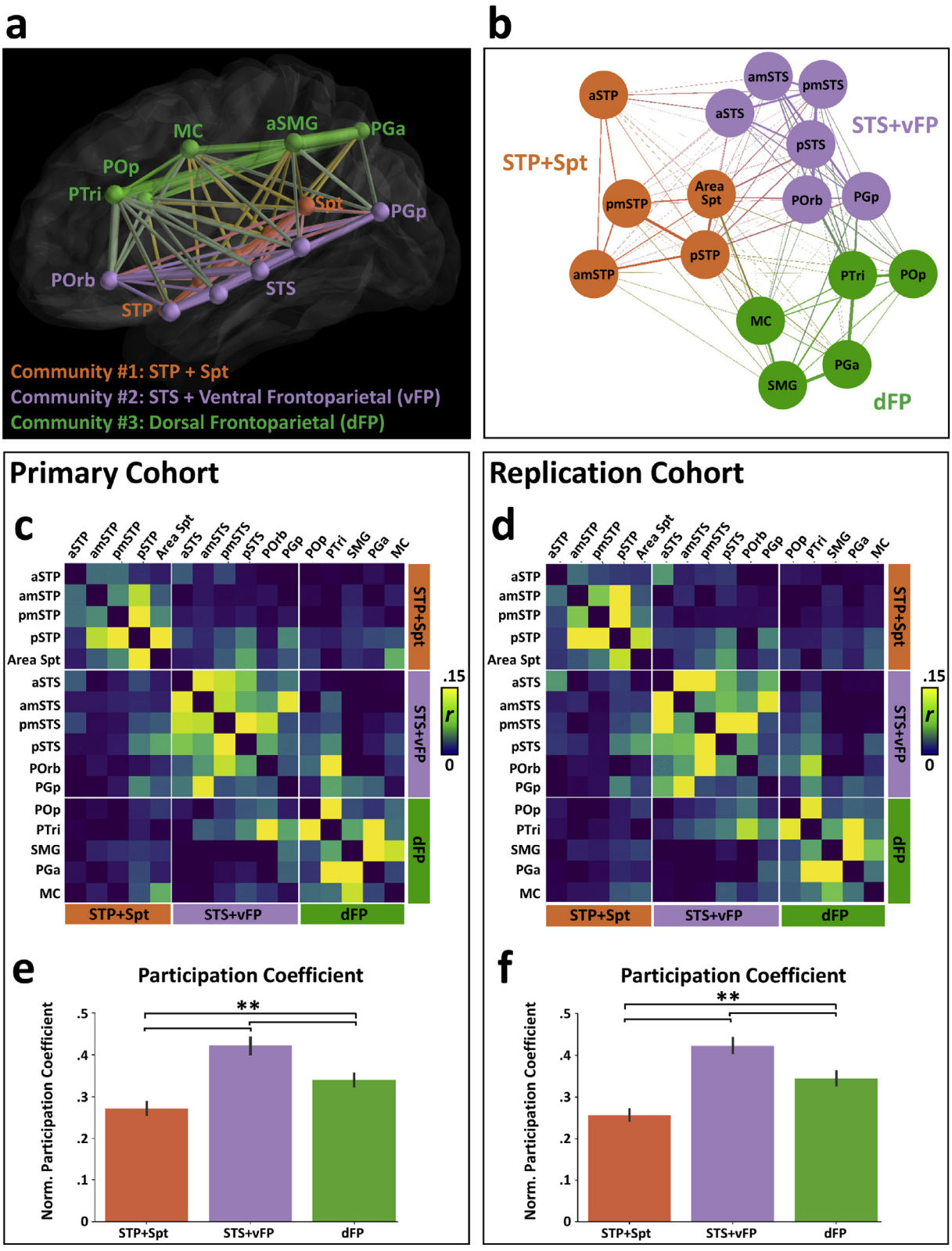

Fig. 1 – Distinct communities within the cortical speech processing network. (a) Community detection analysis shows that STC, IFG, and IPL nodes dissociate into three distinct modules: (1) an STP plus Area Spt module (STP + Spt; orange), (2) an STS plus ventral frontoparietal (vFP) module, which included all STS nodes, pars orbitalis subdivision of the IFG (POrb; Brodmann Area 47), and PGp (STS + vFP; purple), and (3) a dorsal frontoparietal (dFP; green) module that consisted of pars opercularis (POp; Brodmann Area 44), pars triangularis (PTri; Brodmann Area 45), and motor cortex (MC) of frontal cortex and anterior supramarginal gyrus (aSMG) and PGp of parietal cortex. Results from community detection analysis were consistent across primary and replication cohorts. (b) Spring diagram provides an additional visualization of the community

$p \leq .001$, Bonferroni corrected). Results from the omnibus RMANOVA also showed a strong main effect of IFG/IPL target [primary cohort: $F(6, 732) = 54.27$, $p < .0001$; replication cohort: $F(6, 810) = 52.68$, $p < .0001$], and pairwise comparisons showed that POrb of the IFG had greater connectivity compared to POp and MC (primary and replication cohorts: $p < .001$), and PGp had greatest connectivity compared to other parietal target regions (primary and replication cohorts: $p < .0001$).

2.2.2. *Comparing prefrontal and parietal connectivity between STP and Area Spt*

The next goal of the analysis was to test a prediction from a dual-stream model (Hickok & Poeppel, 2007) regarding patterns of connectivity between STP and Area Spt seeds and prefrontal and parietal targets (SI Fig. 2). We first examined STP and Area Spt connectivity with prefrontal targets with a 5 × 4 RMANOVA (STP and Area Spt seeds x Prefrontal targets; see SI Fig. 2a for RMANOVA schematic and results). Results from this analysis showed a main effect of seed [primary cohort: F (4, 488) = 22.80, $p < .0001$; replication cohort: F (4, 540) = 22.22, $p < .0001$], and pairwise comparisons showed greater connectivity between Area Spt and prefrontal targets compared to all STP seeds (primary and replication cohorts: $p \leq .05$). We next examined STP and Area Spt connectivity with parietal targets with a 5 × 3 RMANOVA (STP and Area Spt seeds x Parietal targets; see SI Fig. 2b for RMANOVA schematic and results), and results again showed a main effect of seed [primary cohort: $F(4, 488) = 8.68$, $p < .0001$; replication cohort: F (4, 540) = 6.61, $p = .0002$], and pairwise comparisons showed greater connectivity between Area Spt and parietal targets compared to amSTP and pmSTP seeds (primary and replication cohorts: $p < .01$).

2.2.3. *Comparing prefrontal and parietal connectivity between STS and Area Spt*

While Area Spt showed greater prefrontal and parietal connectivity compared to STP nodes (Results section 2.2.2), omnibus RMANOVA results (Results section 2.2.1) showed a strong effect of STS for prefrontal and parietal connectivity. Therefore, our next goal was to compare the strength of prefrontal and parietal connectivity between STS nodes and Area Spt. Results from 5 × 4 RMANOVA (STS and Area Spt seeds x Prefrontal targets; see SI Fig. 3a for RMANOVA schematic and results) showed a main effect of seed [primary cohort: F (4, 488) = 18.60, $p < .0001$; replication cohort: F (4, 540) = 26.63, $p < .0001$], and pairwise comparisons showed greater connectivity between pSTS and prefrontal targets compared to Area Spt, amSTS, and aSTS (primary and replication cohorts: $p < .01$). Moreover, pmSTS showed greater prefrontal connectivity compared to Area Spt (primary and replication cohorts: $p < .015$). Furthermore, results revealed a significant effect of prefrontal target [primary cohort: F (3, 366) = 34.02, $p < .0001$; replication cohort: F (3, 405) = 50.59, $p < .0001$] and pairwise comparisons showed greater connectivity in POrb of IFG compared to all other prefrontal target regions (primary and replication cohorts: $p \leq .022$). To examine the strength of parietal connectivity between STS nodes and Area Spt, a 5 × 3 RMANOVA was performed (STS and Area Spt seeds x Parietal targets; see SI Fig. 3b for RMANOVA schematic and results). Results showed a significant main effect of seed for the primary cohort [$F(4, 488) = 4.96$, $p = .001$] but not the replication cohort ($p = .10$). Results also revealed a main effect of parietal target [primary cohort: F (2, 244) = 88.90, $p < .0001$; replication cohort: F (2, 270) = 74.22, $p < .0001$] and pairwise comparisons showed greater connectivity in PGp of the IPL compared to aSMG and PGa (primary and replication cohorts: $p < .0001$).

2.2.4. *Connectivity fingerprints*

Connectivity fingerprints were plotted to highlight similarities and differences in prefrontal and parietal connectivity profiles for anterior and posterior STC seeds and Area Spt (Fig. 2d, g). Connectivity fingerprints highlight previous findings by showing: (1) greater connectivity for aSTS compared to aSTP; (2) greater connectivity for pSTS compared to Area Spt; (3) greater POrb connectivity among IFG nodes; and (4) greater PGp connectivity among IPL nodes (Fig. 2d, g).

2.3. *Hemispheric differences in STC functional connectivity profiles*

A final goal of the seed-based functional connectivity analysis was to examine whether there were hemispheric differences in connectivity strength for this temporo-fronto-parietal network.

Hemispheric comparisons: Results from 2 × 2 × 4 × 7 RMANOVA (Hemisphere x STC subregion x Anterior-posterior STC seed location x Prefrontal/Parietal targets) showed a significant main effect of Hemisphere [primary cohort: F (1, 122) = 9.71, $p = .002$; replication cohort: F (1, 135) = 11.48, $p = .001$]; see SI Fig. 4 for RMANOVA schematic and results. Given that previous ANOVA results identified POrb and PGp as primary prefrontal and parietal targets, paired t-tests were then computed to directly examine whether there were connectivity differences between: (a) left versus right-hemisphere STP to ipsilateral POrb and PGp, (b) left versus right-hemisphere STS to ipsilateral POrb and PGp, and (c) left versus right-hemisphere Area Spt to ipsilateral POrb and PGp. Our replicable results demonstrate greater connectivity of left aSTS and amSTS with ipsilateral POrb compared to right-hemisphere aSTS and amSTS homologs (primary and replication cohorts: $p < .001$; Fig. 3c, e, left). Moreover, left-hemisphere amSTS and pmSTS revealed greater connectivity to ipsilateral PGp compared to their right-hemisphere homologs ($p \leq .001$; Fig. 3c, e, right). Finally, right-hemisphere Area Spt revealed greater connectivity to ipsilateral PGp compared to its left-hemisphere homolog ($p < .002$; Fig. 3b, d, rightmost bars).

structure of the speech processing network. Importantly, PGp and POrb serve as connector node linking the STS to other IFG regions. (c–d) Connectivity matrices for the 16 STP, STS, and FP nodes used in the graph analyses. (e–f) Bar graphs show results from participation coefficient analysis. Results reveal that the STS + vFP module has greater normalized participation coefficient among the three communities in the speech processing network. Double asterisks indicate a significant paired t-test ($P < .001$, Bonferroni corrected).

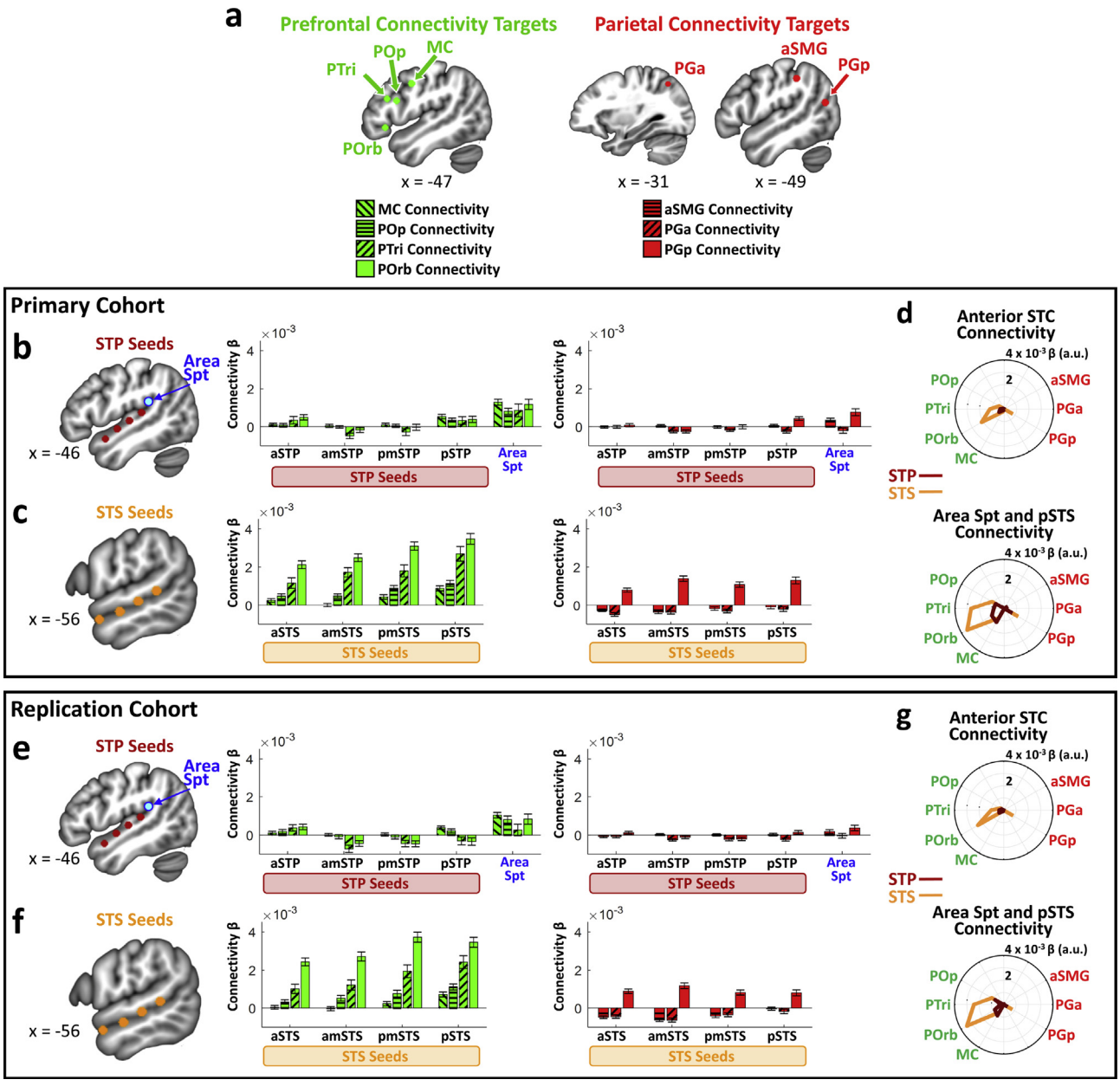

Fig. 2 – Omnibus connectivity results. (a) Anatomy of prefrontal (left; green) and parietal targets (right; red) implicated in speech processing that were examined in the node-wise intrinsic connectivity analysis. (b–d) Primary cohort results: (b) Left: Four STP seeds, extending from posterior to anterior aspects of STC, and Area Spt were used in the seed-based connectivity analysis. Center: Bar graph showing connectivity between STP and Area Spt seeds and four prefrontal target regions. Right: Bar graph showing connectivity between STP and Area Spt seeds and three IPL target regions. Results show weak intrinsic connectivity between STP seeds and IFG and IPL targets implicated in speech perception, with slightly increased connectivity for Area Spt. (c) Left: Four STS seeds, extending from posterior to anterior aspects of STC, were used in the seed-based connectivity analysis. Center: Bar graph showing connectivity between STS seeds and three IFG target regions. Right: Bar graph showing connectivity between STS seeds and three IPL target regions. Results show strong connectivity between multiple STS seeds and IFG targets, particularly for POrb, as well as the PGp of IPL. Similar to STP and Area Spt seed results, STS seeds showed consistently weak connectivity with aSMG and PGa regions of IPL. (d) Top: Connectivity fingerprints show that the aSTS seed (orange) has greater intrinsic connectivity with both IFG and IPL nodes of the speech processing network relative to aSTP (burgundy). Note that the aSTP fingerprints are barely visible given their relatively weak connectivity with IFG and IPL targets. (d) Bottom: Connectivity fingerprints for pSTS (orange) reveal greater prefrontal and parietal connectivity compared to Area Spt. (e–g) Replication cohort results show the same pattern of connectivity for both STP and Area Spt seeds and STS seeds as the Primary cohort. RMANOVA results from both Primary and Replication cohorts indicate a significant main effect of STC subregion, with the STS subregion showing significantly greater overall IFG and IPL connectivity compared to STP ($P < .0001$ for both primary and replication cohorts), and pairwise

3. Discussion

We examined the functional architecture and network organization of brain structures implicated in speech processing. Network stability and consensus analysis revealed a novel tripartite modular organization of the cortical speech processing network. Network stability results further revealed that STS + vFP forms a distinct functional module which serves as a critical link between superior temporal and dorsal frontoparietal circuitry, and suggests its role as a hub in the speech processing network. Consistent with these findings, node-wise connectivity analyses revealed that the STS has a distinct connectivity profile, characterized by greater connectivity to IFG and IPL relative to STP, and greater connectivity with POrb and PGp relative to all other frontoparietal nodes. Importantly, our results represent an advance compared to previous studies as they employ a large sample size, high temporal-resolution fMRI data, and replicability analyses. Our study comprehensively characterizes the circuitry linking temporo-frontal-parietal regions underlying speech processing and suggests that refinement of extant models is required to provide a more coherent synthesis of the speech comprehension network (Binder et al., 2009; Turken & Dronkers, 2011). We first describe the modular architecture revealed by our network analysis, and then discuss our findings in the context of divergent theoretical models in the literature.

3.1. *Modular architecture of the speech processing network*

Network analysis using graph-theoretical procedures provide new information regarding the organization of the speech processing network. Community detection and replication analyses revealed a tripartite functional architecture characterized by distinct STP + Spt, STS + vFP, and dFP modules (Fig. 1). Furthermore, the STS + vFP module has the strongest links to dorsal frontoparietal cortex, and the highest participation coefficient among these three modules, suggesting its role as a hub linking superior temporal to frontoparietal cortex. Results from seed-based analyses further clarify these network findings by showing that a key feature underlying the dissociation between STP + Spt and STS + vFP modules is the enhanced STS connectivity profile with these ventral prefrontal and parietal targets (Fig. 2). Together, results from graph theoretical and seed-based analyses highlight the modular organization of the speech processing network, and the network features underlying functional dissociations within STP and STS subregions of the STC.

Results from community detection analysis further revealed segregation of prefrontal nodes involved in speech processing, highlighting dissociation between POp, PTri, and PMC on the one hand and POrb on the other. Consistent with previous reports (Cole et al., 2013; Crossley et al., 2013), a key feature underlying this segregation is the strong functional coupling between POp, PTri, and MC and the more dorsal parietal nodes of the speech processing network, instantiated in aSMG and PGa (Fig. 1a–d). Importantly, in the domain of speech processing, frontoparietal brain systems are often conceptualized in terms of speech production, particularly POp, PTri, and MC (Flinker et al., 2015; Hickok & Poeppel, 2007). Missing from most models has been POrb, a brain area important for processing semantic and syntactic structure in speech (Abrams et al., 2011; Binder et al., 2009; Friederici, 2015). Our findings point to a clear divergence of prefrontal cortex modular organization: while POp, PTri, and MC form a module with the SMG and PGa, POrb forms a different module with the STS and PGp. The distinct patterns of frontoparietal connectivity are noteworthy because the SMG and PGa, encompassing the more dorso-lateral aspects parietal cortex, have been consistently implicated in verbal working memory (Paulesu, Frith, & Frackowiak, 1993; Ravizza, Delgado, Chein, Becker, & Fiez, 2004) while the PGp, in the posterior-ventral aspect of the angular gyrus, forms part of default mode network regions implicated in inner speech (Binder et al., 2009; Greicius et al., 2003; Uddin et al., 2010). Taken together, this connectivity pattern points to a dissociation in processing streams, with one maintaining short-term working memory for speech and the other linking brain areas involving semantic processing of speech. More generally, findings suggest that conceptualizing frontoparietal circuits in terms of unitary function may be inappropriate, and that a tripartite functional architecture may better capture the known domain-general cognitive functions of frontoparietal cortical regions implicated in speech processing.

3.2. *The STS shows a distinct connectivity profile characterized by enhanced IFG and IPL connectivity*

A major finding of the current study is that, compared to STP, the STS shows a distinct connectivity profile characterized by greater connectivity with prefrontal and parietal targets (Fig. 2). Additionally, STS nodes showed greater prefrontal connectivity relative to Area Spt, a node highlighted in a dual stream model (Hickok & Poeppel, 2007) (SI Fig. 3a). A distinction between STP and STS regions is an important feature of several conceptualizations of the speech processing network (Bates et al., 2003; Binder et al., 2009; Hickok & Poeppel, 2007). These models propose that STP underlies spectrotemporal processing of incoming speech signals, and provides an input for the STS, where phonological analysis of the speech signal is performed (Binder et al., 2000; Liebenthal, Binder, Spitzer, Possing, & Medler, 2005). Our results provide new information by showing that a critical aspect of STP versus STS dissociation is the enhanced prefrontal and parietal connectivity profile of the STS. One interpretation of our connectivity results is that STP and Area Spt provide local processing of speech for spectrotemporal and sensorimotor processing, respectively, however subsequent prefrontal processing relies on a direct connection with the STS. This interpretation is consistent with an influential model stating that the STS is a key node of the speech processing network that connects low-level auditory regions (i.e., STP) with brain systems involved in

comparisons in both cohorts showed greater prefrontal connectivity for pSTS and pmSTS compared to Area Spt ($p < .015$; Bonferroni corrected for multiple comparisons).

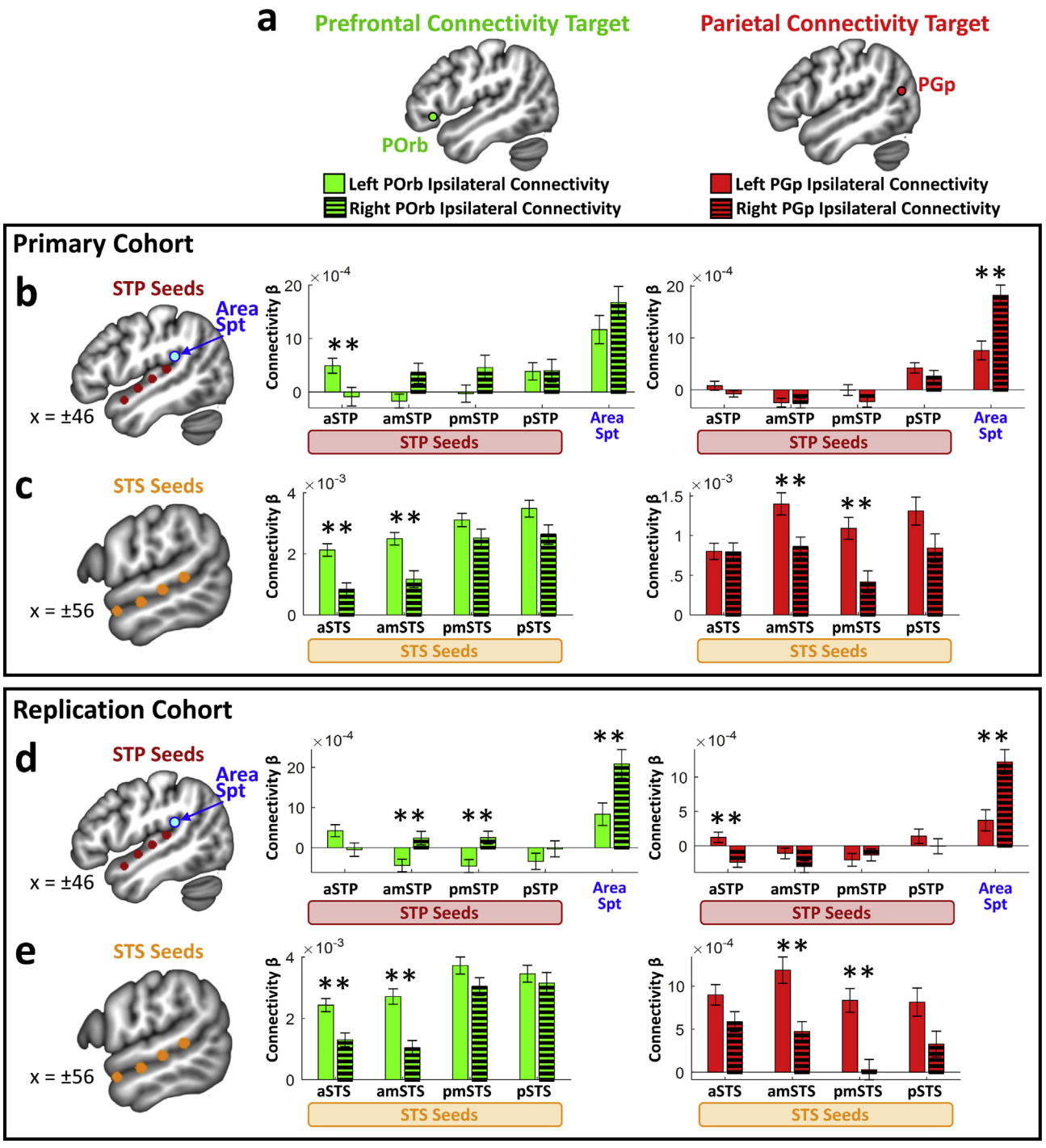

Fig. 3 – Asymmetric connectivity profiles of STC and Area Spt. (a) Anatomy of prefrontal (left; green) and parietal targets (right; red) implicated in speech processing that were examined in the node-wise connectivity analysis. (b–c) Primary cohort results. (b) Left: Four STP seeds, extending from posterior to anterior aspects of STC, and Area Spt were used in the seed-based connectivity analysis. Center: Bar graphs show connectivity of left (solid green) and right STP (green and black stripes) to ipsilateral POrb of IFG for all STP seeds along the anterior-posterior axis of STC. Right: Bar graphs show connectivity of left (solid red) and right STP (red and black stripes) to ipsilateral PGp of IPL for all STP seeds along the anterior-posterior axis of STC. (c) Left: Four STS seeds, extending from posterior to anterior aspects of STC, were used in the seed-based connectivity analysis. Center: Bar graphs show connectivity of left (solid green) and right STS (green and black stripes) to ipsilateral POrb of IFG for all STS seeds along the anterior-posterior axis of STC. Right: Bar graphs show connectivity of left (solid red) and right STS (red and black stripes) to ipsilateral PGp of IPL for all STS seeds along the anterior-posterior axis of STC. Results show that left-hemisphere asymmetry for ipsilateral prefrontal and parietal connections are largely restricted to STS seeds. (d–e) Replication cohort results show similar patterns of connectivity for both STP and Area Spt seeds and STS seeds as the Primary cohort. Double asterisks indicate significant paired t-test ($P < .01$, Bonferroni corrected).

speech, affect, and vocal analysis (Abrams et al., 2016; Abrams, Lynch, et al., 2013; Abrams et al., 2019; Belin, Bestelmeyer, Latinus, & Watson, 2011). Here, we provide additional evidence from connectivity and modularity analyses that the STS serves as a hub in the speech processing network for linking superior temporal regions to lateral prefrontal and parietal targets.

Results also provide new information regarding hierarchical models of auditory cortex. While these models state that STS is at a higher hierarchical level relative to structures of the STP (e.g., belt and parabelt subregions) (Kell, Yamins, Shook, Norman-Haignere, & McDermott, 2018; Leaver & Rauschecker, 2010), they do not identify differential connectivity profiles of distinct prefrontal regions implicated in human speech processing. The current study demonstrates that a prominent feature of the auditory cortical hierarchy is that a hierarchically higher subdivision of auditory cortex, STS, shows greater prefrontal connectivity relative to structures of the STP, encompassing belt and parabelt subdivisions (Sweet, Dorph-Petersen, & Lewis, 2005). Finally, results are consistent with findings from a recent multi-modal parcellation of human cortex, which showed that STS connectivity is distinct from STP regions (Glasser et al., 2016). Here, we characterize key features underlying this distinction by showing that STS has greater connectivity with IFG and IPL nodes compared to STP.

A second major finding is that connectivity profiles of the STS (and STP) are relatively constant for nodes along the anterior-posterior axis of STC, including the ATL (Fig. 3). This result does not support an implicit prediction of one of the dual-stream models, which would predict differential connectivity along the anterior-posterior axis of STC (Rauschecker & Scott, 2009). An interesting question is why do multiple nodes along the anterior-posterior axis of STS have similar access to prefrontal and parietal brain structures? One possibility is that the STS represents a single functional module, which is a reasonable hypothesis given how uniformly this structure is activated during voice-based tasks (Binder et al., 2000; Humphries, Binder, Medler, & Liebenthal, 2007; Obleser, Wise, Dresner, & Scott, 2007). An arguably more plausible explanation is that STS is subdivided into multiple functional units (Deen, Koldewyn, Kanwisher, & Saxe, 2015) that serve different aspects of human speech perception (DeWitt & Rauschecker, 2012), each of which requires similar access to prefrontal and parietal targets.

A third finding with regards to STS connectivity is that the strength of ipsilateral connections between STS and primary prefrontal and parietal targets is greater for left compared to right-hemisphere connections, and leftward asymmetry was specific to STS connectivity profiles. Results are consistent with previous intrinsic connectivity results (Liu, Stufflebeam, Sepulcre, Hedden, & Buckner, 2009) and conceptualizations of the speech processing network (Bates et al., 2003; Binder et al., 2009), and suggest that these asymmetries reflect left-hemisphere dominance for language processes. Our results provide new insights into the lateralization of the human speech processing network by showing that these asymmetries are evident across a wide expanse of STS (but not STP), and that left asymmetric connections are evident in key prefrontal and parietal targets in the speech processing network, including POrb and PGp.

Importantly, findings from intrinsic functional connectivity analyses show convergence with key observations from structural connectivity analyses of lateral temporo-fronto-parietal cortex (Saur et al., 2008; Turken & Dronkers, 2011). Specifically, results from a comprehensive study of the white matter tracts connecting nodes of the speech comprehension network revealed that MTG/STS has a central position within this network characterized by at least five major white matter tracts running beneath it (Turken & Dronkers, 2011). White matter tracts identified in this previous study provide a structural link between many of the key functional connections described in the current study, including: (1) the middle longitudinal fascicle (MdLF), which extends from aSTS through pSTS and ventral portions of AG (likely including PGp), (2) the inferior occipito-frontal fascicle (IOFF), which connects MTG/STS to POrb; (3) the direct segment of the arcuate fasciculus (AF), which makes connections between MTG/STS with dorsal aspects of prefrontal cortex; and (4) the indirect segment of the AF, which connects STS/MTG with lateral aspects of IPL. Together, results from intrinsic functional and structural connectivity analyses (Turken & Dronkers, 2011) provide complementary information and a detailed architecture of the temporo-fronto-parietal speech processing network.

3.3. *POrb is a key connector node linking STS and IFG*

Signaling between left-hemisphere STC and IFG is a core feature in influential cortical models of speech processing. Several models predict a primary role for POp and PTri in speech processing (Bornkessel-Schlesewsky et al., 2015; Friederici, 2012; Hickok & Poeppel, 2007, 2016; Rauschecker & Scott, 2009) and a surprising aspect the current findings is that STS + vFP nodes formed a distinct module within the speech processing network and STS showed significantly greater intrinsic connectivity with POrb relative to POp and PTri. Connectivity results suggests that POrb may serve as a key connector node linking STC with the rest of IFG, a hypothesis that is supported by structural results showing that white matter tracts originating in POrb serve as an input to other IFG structures (Saur et al., 2008). Critically, our findings converge on and extend previous proposals (Friederici, 2015; Saur et al., 2008) by demonstrating that POrb circuits provide a crucial link between STC and POp and PTri, which play a key role in higher-order computations linking the semantic aspects of speech perception with production (Bornkessel-Schlesewsky et al., 2015; Friederici, 2012; Hickok & Poeppel, 2007, 2016; Rauschecker & Scott, 2009).

3.4. *The PGp is a primary parietal target in the speech processing network*

Models of cortical speech processing vary in their view of the contribution of IPL structures to this network (Binder et al., 2009; Dronkers et al., 2004; Tyler & Marslen-Wilson, 2008). Results from seed-based connectivity and network analyses provide new information by showing that the STS has a high degree of intrinsic connectivity with the PGp subdivision of the AG and weaker connectivity with PGa and aSMG. Results are consistent with a previous study which showed that PGp

has greater connectivity with STC compared to PGa (Uddin et al., 2010), and provide new information by showing dissociation between connectivity profiles of PGp and aSMG. Moreover, results from network analyses show an interesting connectivity profile for the aSMG, a structure which has long been associated with language tasks (Petersen, Fox, Posner, Mintun, & Raichle, 1988). Specifically, results identify weak intrinsic connectivity between aSMG and PGp and relatively strong connectivity between aSMG and dorsal IFG regions, including POp and PTri (Fig. 1a). Given SMG's connectivity profile, it remains a distinct possibility that activation of SMG during language tasks is mediated by prefrontal cortex connections rather than by connections from STC to SMG as predicted by some models.

3.5. *Implications for models of speech processing*

An important goal for our study was to examine the intrinsic architecture of temporo-frontal-parietal circuitry as a means of testing key predictions of influential models of speech processing. Notably, extant models make different, and contradictory, sets of predictions regarding functional cortical pathways linking STC and heteromodal target regions (Bornkessel-Schlesewsky et al., 2015; Hickok & Poeppel, 2007; Rauschecker & Scott, 2009). The Rauschecker and Scott dual stream model (Rauschecker & Scott, 2009) proposes: (i) an antero-ventral path, which extends anteriorly from the STC into the POp and PTri, and (ii) a postero-dorsal path, which extends posteriorly from auditory cortex into SMG. Broadly consistent with this model we found strong connectivity of the dorsal IPL nodes with MC and anterior STC connectivity with IFG. However, this model proposes distinct ventral and dorsal processing streams emanating from primary auditory cortex targeting prefrontal and parietal cortical regions, respectively, and results from our analyses did not provide evidence for such pathways. First, network modularity analysis did not reveal separate ventral and dorsal communities along the anterior-posterior axis of STC (Fig. 1a–d). Second, fine-grained seed-based analysis of STP and STS did not reveal greater prefrontal connectivity for anterior versus posterior temporal lobe seeds, nor did it reveal greater parietal connectivity for posterior versus anterior temporal lobe seeds. These findings argue against distinct antero-ventral and posterior-dorsal pathways emanating from primary auditory cortex.

In contrast to the Rauschecker and Scott model, the Hickok and Poeppel's dual stream model (Hickok & Poeppel, 2007) proposes: (i) a ventral stream that originates in primary auditory cortex, descends into more ventral aspects of temporal cortex, and then extends into prefrontal cortex, and (ii) a dorsal stream that encompasses frontoparietal regions instantiated in the IFG, MC, and lateral IPL. Our results are consistent with the ventral stream organization suggested by the Hickok and Poeppel model: we found weak connectivity between STP and IFG while more ventral aspects of temporal cortex (i.e., STS) showed strong connectivity with IFG. Moreover, consistent with the proposed organization of the dorsal stream, we found a high degree of connectivity between frontoparietal brain systems, particularly POp, PTri, MC, and lateral parietal cortex. A key aspect of the Hickok and Poeppel model that was not supported by the current findings is a pronounced role for Area Spt for connecting superior temporal regions to prefrontal and lateral parietal targets. Our analysis revealed that Area Spt had weaker prefrontal and parietal connectivity relative to STS regions and formed a community with STP nodes rather than either prefrontal or parietal nodes. Our findings suggest that POrb in ventral prefrontal cortex together with the STS, rather than Area Spt, are the key connector nodes linking dorsal prefrontal (POp, PTri, MC) and parietal structures (SMG, PGa) in the speech processing network.

Moving beyond these two dual stream models, we observed a strong alignment with speech processing networks based on meta-analyses of speech and language comprehension studies (Binder et al., 2009; Price, 2010) and voxel-based lesion-symptom mapping (Bates et al., 2003; Dronkers et al., 2004). These studies have suggested that: (a) STS, POrb, and PGp are key nodes in the speech processing network; (b) the STS represents a distinct region of STC relative to STP. Results from our connectivity and modularity analyses support these conceptualizations by showing that POrb and PGp are integrated into a community with the STS, and, given that the STS is widely attributed a primary role in speech processing, suggests that POrb and PGp are important nodes in this network. Moreover, community detection results are consistent with the latter hypothesis by identifying the STS as a distinct region of STC relative to STP. Taken together, results from our study replicated across two datasets, help refine and extend key elements of extant models of the human speech processing network.

3.6. *Relating the human speech processing network to behavior*

An important and unanswered question is whether specific features of the speech processing network are related to behavioral aspects of speech production or perception. However, none of the behavioral tasks collected by the HCP are proximal to the study of speech processing (Barch et al., 2013). The closest behavioral tasks in the HCP to the domain of speech processing are Oral Reading Recognition and Picture Vocabulary (Barch et al., 2013), both of which are based on visual rather than auditory stimuli. In the absence of a proximal and easily interpretable measure of speech processing behavior, the current study did not include an analysis of brain-behavior relations. We suggest that future studies will need better behavioral measures to probe the relationship between the functional organization of the speech processing network as identified here and key aspects of speech production and comprehension.

3.7. *Reproducibility in speech neuroscience studies*

Reproducibility represents a major challenge in neuroimaging research, and large sample sizes with replication cohorts have been sparse in previous studies of speech processing. Here we used two large cohorts ($N > 250$) and replicated all reported results. An important direction for future studies is to employ large task-based fMRI datasets to examine how the intrinsic modular architecture identified here regulates speech processing, with a focus on the robustness and replicability of findings.

3.8. Conclusion

In conclusion, we identified several replicable organizational properties of the distributed speech processing network. Our findings, replicated across two cohorts, provide evidence for a tripartite modular architecture of structures supporting speech processing in the human brain. Findings highlight convergence and divergence from current models and strongly suggest that the STS plays a pivotal role in linking STC with prefrontal and parietal brain structures, and that POrb and PGp serve as primary hubs linking STC with frontoparietal circuitry. This model provides a novel and robust template for investigations of how the intrinsic functional architecture of the human speech network is reconfigured during language comprehension and production.

4. Materials and methods

Data acquisition for the HCP was approved by the Institutional Review Board of The Washington University in St. Louis (IRB # 201204036), and all open access data were deidentified.

4.1. Participants

Two cohorts of participants were used in the data analysis and consisted of imaging data collected for the HCP (https://db.humanconnectome.org): primary and replication cohorts. The replication cohort was used to examine robustness and replicability of results using functional brain imaging data collected in a different sample of participants. No part of the procedures or analysis were pre-registered prior to the research being conducted.

We report how we determined our sample size, all data exclusions, all inclusion/exclusion criteria, whether inclusion/exclusion criteria were established prior to data analysis, all manipulations, and all measures in the study. For the primary cohort, minimally-processed resting-state fMRI data were obtained under the HCP 500 data release, and the replication cohort utilized data from participants in the HCP 1200 data release who were not included in the HCP 500 dataset (i.e., none of the participants are in both primary and replication cohorts). Participants were included in the study based on the following criteria: (1) no cortical anatomical abnormalities, reports of instability in the head coil, and prominent artifacts in minimally preprocessed resting-state fMRI data, as reported by HCP (https://wiki.humanconnectome.org/pages/viewpage.action?pageId=88901591); (2) completed the 3T resting-state protocol; (3) average scan-to-scan head motion is less than .2 mm; (4) maximum scan-to-scan head motion is less than 1 mm; (5) handedness ratings $\geq$ 70, indicating strong right-handedness, given that cerebral dominance for language is often reversed in left-handed and ambidextrous individuals; (6) Fluid intelligence (Penn Progressive Matrices, Number of Correct Responses) > mean minus 1 SD based on the HCP 500 sample to include participants in the normal range of intelligence, and (7) English reading ability (Reading Test, Age Adjusted) > mean minus 1 SD based on the HCP 500 sample given that impaired reading is associated with reduced asymmetry of language function (Abrams, Nicol, Zecker, & Kraus, 2006, 2009). These criteria yielded 123 participants (Session 1, left-right encoded, age 22–35, 71 Females, 52 Males) for the primary cohort, and 136 individuals (Session 2, left-right encoded, age 22–35, 67 Females, 69 Males) for the replication cohort.

4.2. Data acquisition

4.2.1. HCP data acquisition

For each individual, 1,200 frames were acquired using multiband, gradient-echo planar imaging with the following parameters: RT, 720 msec; echo time, 33.1 msec; flip angle, 52°; field of view, 280 × 180 mm; matrix, 140 × 90; and voxel dimensions, 2 mm isotropic. During scanning, each individual was eye-fixated on a projected crosshair on the screen.

4.3. Data preprocessing

4.3.1. HCP data preprocessing

Minimally preprocessed resting-state fMRI data were obtained from the HCP. Due to the spatial proximity of the STC Regions of Interest (ROIs), imaging data for the seed-based analyses were not smoothed.

4.4. Experimental design and statistical analysis

The current study examined the functional architecture of temporo-fronto-parietal brain structures implicated in speech processing using complimentary analytic approaches, including: (1) graph theoretic measures to examine network properties of the speech processing network (for more details see the Methods section entitled "***Network stability analysis***"); and (2) seed-based functional connectivity of STC (for more details see the Methods section entitled "***Node-wise functional connectivity analyses***"). The statistical designs for these analyses are described in their respective sub-sections of the Methods as well as the schematics provided in SI Figs. 1–4. All analysis code is available at: https://github.com/scsnl/Abrams_Cortex_2020.

4.5. STC regions of interest

The primary aim of the network stability and seed-based functional connectivity analyses was to probe connectivity strength between STC seed regions and IFG and IPL targets. Specifically, our goal was to examine patterns of IFG and IPL connectivity within and between STC regions, thereby providing information regarding IFG and IPL connectivity across a broad anterior-posterior expanse of STC. Therefore, we constructed seeds which spanned two parallel sub-regions of left-hemisphere STC, including STP and STS (see Fig. 2b. c, Left column, for these anatomical locations).

The STP row consisted of four 4 mm radius adjacent, non-overlapping seeds that extended from posterior (y = −30) through anterior aspects of STP (y = 6). The posterior STP (pSTP) seed was located in the PT (using the Harvard–Oxford probabilistic structural atlas), the posterior medial STP (pmSTP) seed was located in Heschl's gyrus, the anterior medial STP (amSTP) was located in planum polare (PP), and the anterior STP (aSTP) seed was located in the temporal pole

(TP). An additional seed was included for Area Spt, a region located on the border of temporal and parietal cortices identified in a prominent dual-stream model (Hickok & Poeppel, 2007) as a key connector node in the speech processing network. MNI coordinates from a previous study were used to construct a 4 mm radius Area Spt seed (Buchsbaum et al., 2011).

The STS row consisted of four 4 mm adjacent, non-overlapping seeds that extended from posterior aspects of STS (y = −40), just anterior to temporo-occipital cortex, through anterior STS (y = 4) located in the TP. The center coordinates for each seed in the STP and STS rows are listed in SI Table 1.

4.6. IFG and IPL regions of interest

The goal of the network stability and seed-based functional connectivity analysis was to examine the strength of connectivity between STC seeds and circumscribed target areas of IFG and IPL associated with speech-related function. We utilized the NeuroSynth on-line platform (Yarkoni, Poldrack, Nichols, Van Essen, & Wager, 2011) using the search term "Speech" to identify the peak voxel in bilateral IFG, including pars opercularis (POp), pars triangularis (PTri), pars orbitalis (POrb), aSMG, and MC, as defined by the Harvard–Oxford anatomical atlas. NeuroSynth peaks for this search term are shown in SI Table 2. The NeuroSynth peak in the left-hemisphere Harvard–Oxford "Orbital Frontal Cortex" region was located at [−34 24 −4], however this peak overlapped with, and extended into, insular cortex. Therefore, a slightly more lateral peak in POrb, located at [−46, 26, −6], was used in the analysis. 4 mm spheres centered on these peak voxels were then constructed.

An additional goal of the study was to examine the possibility that, consistent with previous reports (Abrams, Ryali, et al., 2013; Davis & Johnsrude, 2003; Evans et al., 2014; Obleser et al., 2007; Peelle et al., 2010), the AG is a primary parietal target for the STC. We therefore constructed 4 mm spheres centered at the peak voxel in the AG for the NeuroSynth search term "Speech." Here the AG is defined as the combined left-hemisphere PGa and PGp subdivisions of the AG, which are based on cytoarchitectonic maps (Caspers et al., 2006). No peak in the NeuroSynth map was present for the right-hemisphere PGp subdivisions. Therefore, the right-hemisphere PGp ROI is defined as the homolog of the left-hemisphere PGp ROI (see SI Table 2).

4.7. Network stability analysis

Functional scans were bandpass filtered in the range .008–0.1Hz, and regional voxel-wise average time series were extracted from each of the 16 ROIs, including 4 STP, 4 STS, Area Spt, 4 prefrontal, and 3 parietal cortex ROIs. Nuisance regressors comprising BOLD signals from the white matter and CSF as well as six rigid-body motion parameters were extracted, bandpass filtered between .008 and 0.1Hz, and regressed from each ROI time series to control for physiological noise and motion artifact. A primary goal of this analysis was to examine functional distinctions among edges and nodes within this network; therefore, partial correlations among residual ROI time series were computed and Fisher's r-to-z transformed to produce a signed, weighted adjacency matrix for each subject. The advantage of using partial, rather than Pearson's, correlations for this analysis is that partial correlations control for the contributions of all other nodes within the specified network (16 ROIs total) prior to calculating the correlation between two nodes of this network. Given the close spatial proximity and established functional relationships between both STC (Binder et al., 2009) and frontoparietal nodes (Corbetta & Shulman, 2002), using partial correlations enables the discovery of unique contributions of each node to the structure of this network (Dwyer et al., 2014).

4.7.1. Community detection

To discover distinct functional modules within this network, we used the Louvain algorithm to maximize Q*, a quality function that enables modularity-based community detection in signed, weighted networks, as implemented in the Brain Connectivity Toolbox [BCT version 2016-01-16, https://sites.google.com/site/bctnet/Home (Rubinov & Sporns, 2010)] for MATLAB. To handle potential degeneracy of community assignments, we repeated this procedure 1000 times in each participant, and averaged the resulting co-classification matrixes to generate a co-occurrence matrix. Subjects' co-occurrence matrices were then averaged to produce a positive, weighted adjacency, and a consensus partition at the group level was determined using the method of (Lancichinetti & Fortunato, 2012) with tau = .1 and 1000 iterations.

4.7.2. Participation coefficient

To investigate the centrality of nodes in the network, we computed participation coefficient, which measures the distribution of a node's edges among the communities identified in a network (Power, Schlaggar, & Petersen, 2014). We computed participation coefficient in each participant across a range of density thresholds from 5% to 20% and averaged measures across thresholds for each node within each participant. To account for the known module size bias in PC, the method recently proposed by Pedersen et al. was used to compute normalized participation coefficient (Pedersen, Omidvarnia, Shine, Jackson, & Zalesky, 2019). Briefly, for each subject, 1000 surrogate connectivity matrices were generated using the "*null_model_und_sign*" function from the Brain Connectivity Toolbox, which preserved the degree, weight, and strength distributions per node. These surrogate connectivity matrices were used to normalize the node-to-module degree value in the participation coefficient equation as described in Pedersen et al. Normalized PC values averaged within each module are plotted in Fig. 1e–f. Paired samples *t*-tests were then conducted to examine differences in normalized participation coefficient for each community.

4.8. Node-wise functional connectivity analyses

For each ROI, a resting-state time series was extracted by averaging the time series of all voxels within it. The resulting ROI time series was then used as a covariate of

interest in a linear regression whole-brain analysis. A global time series computed across all brain voxels, along with six motion parameters, were used as additional covariates to remove confounding effects of physiological noise and participant movement. Intrinsic connectivity between the STC seeds and the IFG and IPL target regions were calculated as the mean beta value within these spherical targets for each STC seed.

Repeated measures ANOVAs (RMANOVA) were used to quantify connectivity differences between different seed regions and target combinations. Mean beta values within specific IFG and IPL target regions were calculated from individual subject contrast images from the STC-seeded whole-brain connectivity analyses. Individual subjects' mean beta values were then exported to SPSS (SPSS Inc., Chicago, IL, USA) where four RMANOVAs were performed:

1. An omnibus 2 × 4 × 7 RMANOVA with factors (1) STC subregion (i.e., STP *vs* STS), (2) Anterior-poster STC seed location, and (3) Prefrontal/Parietal target was performed (see top of SI Fig. 1 for schematic). This omnibus ANOVA design allowed us to separately examine multiple aspects of STC connectivity, including differential connectivity between STP and STS subregions, anterior versus posterior aspects of STC, and their connectivity profiles with key IFG and IPL targets. Results from this analysis are reported in section 2.2.1 Main Effects.
2. To examine differential patterns of prefrontal and parietal connectivity between STP and Area Spt seeds, two RMANOVAs were performed, including: (1) STP and Area Spt seeds x Prefrontal connectivity, and (2) STP and Area Spt seeds x Parietal connectivity (see top of SI Fig. 2a, b for schematics). Results from this analysis are reported in section 2.2.2 Comparing prefrontal and parietal connectivity between STP and Area Spt.
3. To examine differential patterns of prefrontal and parietal connectivity between STS and Area Spt seeds, two RMANOVAs were performed, including: (1) STS and Area Spt seeds x Prefrontal connectivity, and (2) STS and Area Spt seeds x Parietal connectivity (see top of SI Fig. 3a, b for schematics). Results from this analysis are reported in section 2.2.3 Comparing prefrontal and parietal connectivity between STS and Area Spt.
4. To examine hemispheric differences in STC functional connectivity profiles for ipsilateral prefrontal and parietal connections, a 2 × 2 × 4 × 7 RMANOVA with factors (1) hemisphere (left *vs* right), (2) STC subregion (i.e., STP *vs* STS), (3) Anterior-poster STC seed location, and (4) IFG/IPL target was performed (see top of SI Fig. 4 for schematic). Results from this analysis are reported in section 2.3 Hemispheric differences in STC functional connectivity profiles Hemispheric comparisons.

When RMANOVAs violated assumptions of sphericity, Greenhouse-Geisser correction was applied to the reported results, and *p*-values for all pair-wise comparisons of seeds and targets were Bonferroni adjusted for multiple comparisons.

An additional *post-hoc* analysis was performed to probe hemispheric asymmetries. To examine hemispheric asymmetries for ipsilateral connections between STC and Area Spt seed regions and representative prefrontal (i.e., POrb) and parietal targets (i.e., PGp), paired *t*-tests were computed between: (a) left versus right-hemisphere STP seeds to ipsilateral POrb and PGp, (b) left versus right-hemisphere STS seeds to ipsilateral POrb and PGp, and (c) left versus right-hemisphere Area Spt to ipsilateral POrb and PGp. All *t*-tests were Bonferroni corrected for multiple comparisons.

Author contributions

Daniel A. Abrams: Conceptualization, Methodology, Software, Writing - Original draft preparation, Writing - Review & Editing, Visualization, Formal analysis, Project administration.

John Kochalka: Methodology, Software, Visualization, Formal analysis, Data Curation.

Sayuli Bhide: Methodology, Formal analysis.

Srikanth Ryali: Methodology, Formal analysis.

Vinod Menon: Conceptualization, Writing - Review & Editing, Project administration.

D.A.A. and V.M. designed research; D.A.A., J.K., S.R., and V.M. contributed new reagents/analytic tools; D.A.A., J.K., S.B., and S.R. analyzed data; and D.A.A. and V.M. wrote the paper.

Open practices

The study in this article earned an Open Data – Protected Access badge for transparent practices. Materials and data for the study are available at https://db.humanconnectome.org.

Declaration of Competing Interest

The authors declare no competing financial interest.

Acknowledgments

This work was supported by National Institutes of Health Grants (grant numbers K01MH102428 to D.A.A, K25HD074652 to S.R., and DC011095 and MH084164 to V.M.); a NARSAD Young Investigator Grant from the Brain and Behavior Research Foundation (to D.A.A.), the Singer Foundation; and the Simons Foundation for Autism Research (308939 to V.M.). Data were provided by the Human Connectome Project, WU-Minn Consortium (Principal Investigators: David Van Essen and Kamil Ugurbil; 1U54MH091657) funded by the 16 NIH Institutes and Centers that support the NIH Blueprint for Neuroscience Research; and by the McDonnell Center for Systems Neuroscience at Washington University. We thank T. Evans for useful discussions regarding this work and T. Chen for technical assistance.

Supplementary data

Supplementary data to this article can be found online at https://doi.org/10.1016/j.cortex.2020.03.013.

REFERENCES

Abrams, D. A., Bhatara, A., Ryali, S., Balaban, E., Levitin, D. J., & Menon, V. (2011). Decoding temporal structure in music and speech relies on shared brain resources but elicits different fine-scale spatial patterns. *Cerebral Cortex, 21*(7), 1507–1518. https://doi.org/10.1093/cercor/bhq198.

Abrams, D. A., Chen, T., Odriozola, P., Cheng, K. M., Baker, A. E., Padmanabhan, A., et al. (2016). Neural circuits underlying mother's voice perception predict social communication abilities in children. *Proceedings of the National Academy of Sciences of the United States of America, 113*(22), 6295–6300. https://doi.org/10.1073/pnas.1602948113.

Abrams, D. A., Lynch, C. J., Cheng, K. M., Phillips, J., Supekar, K., Ryali, S., et al. (2013). Underconnectivity between voice-selective cortex and reward circuitry in children with autism. *Proceedings of the National Academy of Sciences of the United States of America, 110*(29), 12060–12065. https://doi.org/10.1073/pnas.1302982110.

Abrams, D. A., Nicol, T., Zecker, S. G., & Kraus, N. (2006). Auditory brainstem timing predicts cerebral asymmetry for speech. *Journal of Neuroscience, 26*(43), 11131–11137. https://doi.org/10.1523/JNEUROSCI.2744-06.2006.

Abrams, D. A., Nicol, T., Zecker, S., & Kraus, N. (2009). Abnormal cortical processing of the syllable rate of speech in poor readers. *Journal of Neuroscience, 29*(24), 7686–7693. https://doi.org/10.1523/JNEUROSCI.5242-08.2009.

Abrams, D. A., Padmanabhan, A., Chen, T., Odriozola, P., Baker, A. E., Kochalka, J., et al. (2019). Impaired voice processing in reward and salience circuits predicts social communication in children with autism. *Elife, 8*. https://doi.org/10.7554/eLife.39906.

Abrams, D. A., Ryali, S., Chen, T., Balaban, E., Levitin, D. J., & Menon, V. (2013). Multivariate activation and connectivity patterns discriminate speech intelligibility in Wernicke's, Broca's, and Geschwind's areas. *Cerebral Cortex, 23*(7), 1703–1714. https://doi.org/10.1093/cercor/bhs165.

Barch, D. M., Burgess, G. C., Harms, M. P., Peterson, S. E., Schlaggar, B. L., Corbetta, M., et al. (2013). Function in the human connectome: Task-fMRI and individual differences in behavior. *NeuroImage, 80*, 169–189. https://doi.org/10.1016/j.neuroimage.2013.05.033.

Bates, E., Wilson, S. M., Saygin, A. P., Dick, F., Sereno, M. I., Knight, R. T., et al. (2003). Voxel-based lesion-symptom mapping. *Nature Neuroscience, 6*(5), 448–450. https://doi.org/10.1038/nn1050.

Belin, P., Bestelmeyer, P. E., Latinus, M., & Watson, R. (2011). Understanding voice perception. *British Journal of Psychology, 102*(4), 711–725. https://doi.org/10.1111/j.2044-8295.2011.02041.x.

Binder, J. R., Desai, R. H., Graves, W. W., & Conant, L. L. (2009). Where is the semantic system? A critical review and meta-analysis of 120 functional neuroimaging studies. *Cerebral Cortex, 19*(12), 2767–2796. https://doi.org/10.1093/cercor/bhp055.

Binder, J. R., Frost, J. A., Hammeke, T. A., Bellgowan, P. S., Springer, J. A., Kaufman, J. N., et al. (2000). Human temporal lobe activation by speech and nonspeech sounds. *Cerebral Cortex, 10*(5), 512–528.

Bornkessel-Schlesewsky, I., Schlesewsky, M., Small, S. L., & Rauschecker, J. P. (2015). Neurobiological roots of language in primate audition: Common computational properties. *Trends in Cognitive Sciences, 19*(3), 142–150. https://doi.org/10.1016/j.tics.2014.12.008.

Bressler, S. L., & Menon, V. (2010). Large-scale brain networks in cognition: Emerging methods and principles. *Trends in Cognitive Sciences, 14*(6), 277–290. https://doi.org/10.1016/j.tics.2010.04.004.

Buchsbaum, B. R., Baldo, J., Okada, K., Berman, K. F., Dronkers, N., D'Esposito, M., et al. (2011). Conduction aphasia, sensory-motor integration, and phonological short-term memory - an aggregate analysis of lesion and fMRI data. *Brain and Language, 119*(3), 119–128. https://doi.org/10.1016/j.bandl.2010.12.001.

Buchsbaum, B. R., Hickok, G., & Humphries, C. (2001). Role of left posterior superior temporal gyrus in phonological processing for speech perception and production. *Cognitive Science, 25*(5), 663–678.

Buchsbaum, B. R., Olsen, R. K., Koch, P., & Berman, K. F. (2005). Human dorsal and ventral auditory streams subserve rehearsal-based and echoic processes during verbal working memory. *Neuron, 48*(4), 687–697. https://doi.org/10.1016/j.neuron.2005.09.029.

Bullmore, E., & Sporns, O. (2009). Complex brain networks: Graph theoretical analysis of structural and functional systems. *Nature Reviews Neuroscience, 10*(3), 186–198.

Cai, W., Ryali, S., Chen, T., Li, C. S., & Menon, V. (2014). Dissociable roles of right inferior frontal cortex and anterior insula in inhibitory control: Evidence from intrinsic and task-related functional parcellation, connectivity, and response profile analyses across multiple datasets. *Journal of Neuroscience, 34*(44), 14652–14667. https://doi.org/10.1523/JNEUROSCI.3048-14.2014.

Caspers, S., Geyer, S., Schleicher, A., Mohlberg, H., Amunts, K., & Zilles, K. (2006). The human inferior parietal cortex: Cytoarchitectonic parcellation and interindividual variability. *Neuroimage, 33*(2), 430–448. https://doi.org/10.1016/j.neuroimage.2006.06.054.

Cole, M. W., Reynolds, J. R., Power, J. D., Repovs, G., Anticevic, A., & Braver, T. S. (2013). Multi-task connectivity reveals flexible hubs for adaptive task control. *Nature Neuroscience, 16*(9), 1348–1355. https://doi.org/10.1038/nn.3470.

Corbetta, M., & Shulman, G. L. (2002). Control of goal-directed and stimulus-driven attention in the brain. *Nature Reviews Neuroscience, 3*(3), 201–215. https://doi.org/10.1038/nrn755.

Crossley, N. A., Mechelli, A., Vertes, P. E., Winton-Brown, T. T., Patel, A. X., Ginestet, C. E., et al. (2013). Cognitive relevance of the community structure of the human brain functional coactivation network. *Proceedings of the National Academy of Sciences of the United States of America, 110*(28), 11583–11588. https://doi.org/10.1073/pnas.1220826110.

Davis, M. H., & Johnsrude, I. S. (2003). Hierarchical processing in spoken language comprehension. *Journal of Neuroscience, 23*(8), 3423–3431.

Deen, B., Koldewyn, K., Kanwisher, N., & Saxe, R. (2015). Functional organization of social perception and cognition in the superior temporal sulcus. *Cerebral Cortex, 25*(11), 4596–4609. https://doi.org/10.1093/cercor/bhv111.

DeWitt, I., & Rauschecker, J. P. (2012). Phoneme and word recognition in the auditory ventral stream. *Proceedings of the National Academy of Sciences of the United States of America, 109*(8), E505–E514. https://doi.org/10.1073/pnas.1113427109.

Dronkers, N. F., Wilkins, D. P., Van Valin, R. D., Jr., Redfern, B. B., & Jaeger, J. J. (2004). Lesion analysis of the brain areas involved in language comprehension. *Cognition, 92*(1–2), 145–177. https://doi.org/10.1016/j.cognition.2003.11.002.

Dwyer, D. B., Harrison, B. J., Yucel, M., Whittle, S., Zalesky, A., Pantelis, C., et al. (2014). Large-scale brain network dynamics supporting adolescent cognitive control. *Journal of Neuroscience, 34*(42), 14096–14107. https://doi.org/10.1523/JNEUROSCI.1634-14.2014.

Evans, S., Kyong, J. S., Rosen, S., Golestani, N., Warren, J. E., McGettigan, C., et al. (2014). The pathways for intelligible speech: Multivariate and univariate perspectives. *Cerebral Cortex, 24*(9), 2350–2361. https://doi.org/10.1093/cercor/bht083.

Flinker, A., Korzeniewska, A., Shestyuk, A. Y., Franaszczuk, P. J., Dronkers, N. F., Knight, R. T., et al. (2015). Redefining the role of Broca's area in speech. *Proceedings of the National Academy of*

Sciences of the United States of America, 112(9), 2871–2875. https://doi.org/10.1073/pnas.1414491112.
Fridriksson, J., Yourganov, G., Bonilha, L., Basilakos, A., Den Ouden, D. B., & Rorden, C. (2016). Revealing the dual streams of speech processing. *Proceedings of the National Academy of Sciences of the United States of America, 113*(52), 15108–15113. https://doi.org/10.1073/pnas.1614038114.
Friederici, A. D. (2012). The cortical language circuit: From auditory perception to sentence comprehension. *Trends in Cognitive Sciences, 16*(5), 262–268. https://doi.org/10.1016/j.tics.2012.04.001.
Friederici, A. D. (2015). White-matter pathways for speech and language processing. *Handbook of Clinical Neurology, 129*, 177–186. https://doi.org/10.1016/B978-0-444-62630-1.00010-X.
Geschwind, N. (1970). The organization of language and the brain. *Science, 170*(3961), 940–944.
Glasser, M. F., Coalson, T. S., Robinson, E. C., Hacker, C. D., Harwell, J., Yacoub, E., et al. (2016). A multi-modal parcellation of human cerebral cortex. *Nature, 536*(7615), 171–178. https://doi.org/10.1038/nature18933.
Greicius, M. D., Krasnow, B., Reiss, A. L., & Menon, V. (2003). Functional connectivity in the resting brain: A network analysis of the default mode hypothesis. *Proceedings of the National Academy of Sciences of the United States of America, 100*(1), 253–258. https://doi.org/10.1073/pnas.0135058100.
Hickok, G., & Poeppel, D. (2007). The cortical organization of speech processing. *Nature Reviews Neuroscience, 8*(5), 393–402. https://doi.org/10.1038/nrn2113.
Hickok, G., & Poeppel, D. (2016). *Neural basis of speech perception Neurobiology of Language* (pp. 299–310). Elsevier.
Humphries, C., Binder, J. R., Medler, D. A., & Liebenthal, E. (2007). Time course of semantic processes during sentence comprehension: An fMRI study. *Neuroimage, 36*(3), 924–932. https://doi.org/10.1016/j.neuroimage.2007.03.059.
Kell, A. J. E., Yamins, D. L. K., Shook, E. N., Norman-Haignere, S. V., & McDermott, J. H. (2018). A task-optimized neural network replicates human auditory behavior, predicts brain Responses, and reveals a cortical processing hierarchy. *Neuron, 98*(3), 630–644. https://doi.org/10.1016/j.neuron.2018.03.044.
Lancichinetti, A., & Fortunato, S. (2012). Consensus clustering in complex networks. *Scientific Reports, 2*, 336. https://doi.org/10.1038/srep00336.
Leaver, A. M., & Rauschecker, J. P. (2010). Cortical representation of natural complex sounds: Effects of acoustic features and auditory object category. *Journal of Neuroscience, 30*(22), 7604–7612. https://doi.org/10.1523/Jneurosci.0296-10.2010.
Liebenthal, E., Binder, J. R., Spitzer, S. M., Possing, E. T., & Medler, D. A. (2005). Neural substrates of phonemic perception. *Cerebral Cortex, 15*(10), 1621–1631. https://doi.org/10.1093/cercor/bhi040.
Liu, H., Stufflebeam, S. M., Sepulcre, J., Hedden, T., & Buckner, R. L. (2009). Evidence from intrinsic activity that asymmetry of the human brain is controlled by multiple factors. *Proceedings of the National Academy of Sciences of the United States of America, 106*(48), 20499–20503. https://doi.org/10.1073/pnas.0908073106.
Mishkin, M., Ungerleider, L. G., & Macko, K. A. (1983). Object vision and spatial vision - 2 cortical pathways. *Trends in Neurosciences, 6*(10), 414–417. https://doi.org/10.1016/0166-2236(83)90190-X.
Obleser, J., Wise, R. J., Dresner, M. A., & Scott, S. K. (2007). Functional integration across brain regions improves speech perception under adverse listening conditions. *Journal of Neuroscience, 27*(9), 2283–2289. https://doi.org/10.1523/JNEUROSCI.4663-06.2007.
Paulesu, E., Frith, C. D., & Frackowiak, R. S. (1993). The neural correlates of the verbal component of working memory. *Nature, 362*(6418), 342–345. https://doi.org/10.1038/362342a0.
Pedersen, M., Omidvarnia, A., Shine, J. M., Jackson, G. D., & Zalesky, A. (2019). Reducing module size bias of participation coefficient. *bioRxiv*, 747162.
Peelle, J. E., Johnsrude, I. S., & Davis, M. H. (2010). Hierarchical processing for speech in human auditory cortex and beyond. *Frontiers in Human Neuroscience, 4*, 51. https://doi.org/10.3389/fnhum.2010.00051.
Petersen, S. E., Fox, P. T., Posner, M. I., Mintun, M., & Raichle, M. E. (1988). Positron emission tomographic studies of the cortical anatomy of single-word processing. *Nature, 331*(6157), 585–589. https://doi.org/10.1038/331585a0.
Power, J. D., Cohen, A. L., Nelson, S. M., Wig, G. S., Barnes, K. A., Church, J. A., et al. (2011). Functional network organization of the human brain. *Neuron, 72*(4), 665–678. https://doi.org/10.1016/j.neuron.2011.09.006.
Power, J. D., Schlaggar, B. L., & Petersen, S. E. (2014). Studying brain organization via spontaneous fMRI signal. *Neuron, 84*(4), 681–696. https://doi.org/10.1016/j.neuron.2014.09.007.
Price, C. J. (2010). The anatomy of language: A review of 100 fMRI studies published in 2009. *Annals of the New York Academy of Sciences, 1191*, 62–88. https://doi.org/10.1111/j.1749-6632.2010.05444.x.
Rauschecker, J. P., & Scott, S. K. (2009). Maps and streams in the auditory cortex: Nonhuman primates illuminate human speech processing. *Nature Neuroscience, 12*(6), 718–724. https://doi.org/10.1038/nn.2331.
Rauschecker, J. P., & Tian, B. (2000). Mechanisms and streams for processing of "what" and "where" in auditory cortex. *Proceedings of the National Academy of Sciences of the United States of America, 97*(22), 11800–11806. https://doi.org/10.1073/pnas.97.22.11800.
Ravizza, S. M., Delgado, M. R., Chein, J. M., Becker, J. T., & Fiez, J. A. (2004). Functional dissociations within the inferior parietal cortex in verbal working memory. *Neuroimage, 22*(2), 562–573. https://doi.org/10.1016/j.neuroimage.2004.01.039.
Rubinov, M., & Sporns, O. (2010). Complex network measures of brain connectivity: Uses and interpretations. *Neuroimage, 52*(3), 1059–1069. https://doi.org/10.1016/j.neuroimage.2009.10.003.
Saur, D., Kreher, B. W., Schnell, S., Kummerer, D., Kellmeyer, P., Vry, M. S., et al. (2008). Ventral and dorsal pathways for language. *Proceedings of the National Academy of Sciences of the United States of America, 105*(46), 18035–18040. https://doi.org/10.1073/pnas.0805234105.
Scott, S. K., Blank, C. C., Rosen, S., & Wise, R. J. S. (2000). Identification of a pathway for intelligible speech in the left temporal lobe. *Brain, 123*, 2400–2406. https://doi.org/10.1093/brain/123.12.2400.
Seeley, W. W., Menon, V., Schatzberg, A. F., Keller, J., Glover, G. H., Kenna, H., et al. (2007). Dissociable intrinsic connectivity networks for salience processing and executive control. *Journal of Neuroscience, 27*(9), 2349–2356. https://doi.org/10.1523/JNEUROSCI.5587-06.2007.
Supekar, K., Uddin, L. Q., Khouzam, A., Phillips, J., Gaillard, W. D., Kenworthy, L. E., et al. (2013). Brain hyperconnectivity in children with autism and its links to social deficits. *Cell Reports, 5*(3), 738–747. https://doi.org/10.1016/j.celrep.2013.10.001.
Sweet, R. A., Dorph-Petersen, K. A., & Lewis, D. A. (2005). Mapping auditory core, lateral belt, and parabelt cortices in the human superior temporal gyrus. *Journal of Comparative Neurology, 491*(3), 270–289. https://doi.org/10.1002/cne.20702.
Turken, A. U., & Dronkers, N. F. (2011). The neural architecture of the language comprehension network: Converging evidence from lesion and connectivity analyses. *Frontiers in Systems Neuroscience, 5*, 1. https://doi.org/10.3389/fnsys.2011.00001.

Tyler, L. K., & Marslen-Wilson, W. (2008). Fronto-temporal brain systems supporting spoken language comprehension. *Philosophical Transactions of the Royal Society of London B Biological Sciences, 363*(1493), 1037–1054. https://doi.org/10.1098/rstb.2007.2158.

Uddin, L. Q., Supekar, K., Amin, H., Rykhlevskaia, E., Nguyen, D. A., Greicius, M. D., et al. (2010). Dissociable connectivity within human angular gyrus and intraparietal sulcus: Evidence from functional and structural connectivity. *Cerebral Cortex, 20*(11), 2636–2646. https://doi.org/10.1093/cercor/bhq011.

Van Essen, D. C., Smith, S. M., Barch, D. M., Behrens, T. E., Yacoub, E., Ugurbil, K., et al. (2013). The WU-Minn human connectome Project: An overview. *Neuroimage, 80*, 62–79. https://doi.org/10.1016/j.neuroimage.2013.05.041.

Wernicke, C. (1874). *Der Aphasische Symptomencomplex*. Breslau: Cohn and Weigert.

Yarkoni, T., Poldrack, R. A., Nichols, T. E., Van Essen, D. C., & Wager, T. D. (2011). Large-scale automated synthesis of human functional neuroimaging data. *Nature Methods, 8*(8), 665–670. https://doi.org/10.1038/nmeth.1635.